



La doping effect on TZM alloy oxidation behavior



Fan Yang^a, Kuai-She Wang^{a,*}, Ping Hu^a, Huan-Cheng He^a, Xuan-Qi Kang^a, Hua Wang^b, Ren-Zhi Liu^{a,c}, Alex A. Volinsky^d

^aSchool of Metallurgy Engineering, Xi'an University of Architecture and Technology, Xi'an 710055, China

^bXi'an Electric Furnace Institute Co., Ltd., Xi'an 710061, China

^cJinduicheng Molybdenum Co., Ltd., Xi'an 710068, China

^dDepartment of Mechanical Engineering, University of South Florida, Tampa FL 33620, USA

ARTICLE INFO

Article history:

Received 11 October 2013

Received in revised form 18 December 2013

Accepted 19 December 2013

Available online 13 January 2014

Keywords:

La doping

TZM alloy

Oxidation behavior

Oxidation coating

ABSTRACT

Powder metallurgy methods were utilized to prepare lanthanum-doped (La-TZM) and traditional TZM alloy plates. High temperature oxidation experiments along with the differential thermal analysis were employed to study the oxidation behavior of the two kinds of TZM alloys. An extremely volatile oxide layer was generated on the surface of traditional TZM alloy plates when the oxidation started. Molybdenum oxide volatilization exposed the alloy matrix, which was gradually corroded by oxygen, losing its quality with serious surface degradation. The La-TZM alloy has a more compact structure due to the lanthanum doping. The minute lanthanum oxide particles are pinned at the grain boundaries and refine the grains. Oxide layer generated on the matrix surface can form a compact coating, which effectively blocks the surface from being corroded by oxidation. The oxidation resistance of La-TZM alloys has been enhanced, expanding its application range.

© 2014 Elsevier B.V. All rights reserved.

1. Introduction

TZM molybdenum alloy contains 0.5–0.8 wt% titanium, 0.08–0.1 wt% zirconium, 0.016–0.02 wt% carbon and molybdenum balance. Molybdenum TZM alloys are highly desirable for a wide range of critical applications due to their high electrical and thermal conductivity, strength and creep resistance at elevated temperatures, high temperature stability, low coefficient of thermal expansion and excellent corrosion resistance in liquid metals [1–7]. They are widely used in aerospace, power generation, nuclear and fusion reactors, military, industrial and chemical applications, where these alloys are subjected to high temperatures, liquid metal corrosion and other aggressive environments. However, poor high temperature oxidation resistance in the presence of air has restricted TZM alloys practical applications. Research shows that when the temperature is below 400 °C, the oxidation rate of TZM alloys is very low. When the temperature is between 400 °C and 650 °C, the mass gain by oxidation is rapidly increased, generating MoO₂ and other oxides (MoO_z, 2 < z < 3). When temperature raises above 650 °C, a sharp decline in mass will happen due to the MoO₃ volatilization [8].

Previous studies have shown that doping lanthanum into traditional TZM alloy can significantly improve its strength and toughness [9]. This article investigates the effect of lanthanum doping on the oxidation behavior of TZM alloy plates.

2. Experimental procedure

2.1. Preparation of TZM and La-TZM alloys

Based on the design composition, listed in Table 1, two kinds of TZM alloys were prepared: La-doped TZM alloy (#1) and traditional TZM alloy (#2). Adopting the solid–liquid mixing process, stearic acid ethanol solution containing lanthanum nitrate, was used along with TiH₂ and ZrH₂ powders to obtain lanthanum-doped Mo. By the processes of mixing, ball-milling (using planetary ball milling machine, revolving speed 240 r/min, milling 2 h), vacuum drying (using vacuum drying oven, 70 °C, 4 h), compaction (holding pressure 21 MPa, 5 s) and sintering (pass into protective hydrogen, subsection sintering: 300 °C, 900 °C, 1200 °C heat preservation 2 h respectively, finally sintering on 1900 °C, heat preservation 4 h), both La-TZM and TZM alloy compacts were obtained. La-TZM and TZM alloy plates, 0.5 mm thick, were made by hot-rolling, warm-rolling and caustic washing. The plates were separately cut into 4 pieces, labeled as samples of #1-1, #1-2, #2-1 and #2-2.

2.2. High temperature oxidation experiments

During the high temperature oxidation experiments, La-TZM and TZM alloy plates (samples #1-1 and #2-1) were heated at 300 °C, 450 °C, 600 °C, 800 °C, and 1000 °C in the furnace for 10 min, 15 min and 30 min. Electronic balance was used to measure the sample mass (0.01 g accuracy) before and after heating to calculate the samples mass loss.

2.3. Samples characterization

JSM-6460LV scanning electron microscope (JEOL, Japan) was used for the surface and cross-sectional morphology, and microstructure characterization of the samples after high temperature oxidation. Energy dispersive spectra (EDS) analyzer was used to obtain the surface composition.

* Corresponding author. Tel.: +86 29 82205096; fax: +86 29 82202923.

E-mail address: wangkuaish888@126.com (K.-S. Wang).

Table 1
Composition of TZM alloys (wt%).

Sample	Ti	Zr	C	Stearic acid	La(NO ₃) ₃	Mo
#1	0.5	0.1	0	0.25	1.99	Balance
#2	0.5	0.1	0	0.25	0	Balance

2.4. Comprehensive thermal analysis

Differential thermal analysis (DTA) and thermogravimetry (TG) experiments were conducted with sample #1-2 and #2-2 in air by using the HQC-3 differential thermal analyzer (Hengjiu Co., Beijing China). The temperature was varied from room temperature to 1100 °C with 25 °C/min heating rate. The DTA–TG curves were used to analyze the thermogravimetric loss and the reaction mechanism.

3. Results and discussion

3.1. Oxidation kinetics of La-TZM and TZM alloys

Fig. 1 shows the oxidation mass loss of La-TZM and TZM alloy plates of the same size, heated for 10 min, 15 min and 30 min using the same conditions. There is no mass change of La-TZM and TZM alloy plates under 600 °C, indicating no obvious oxidation. Past 600 °C the mass loss increases linearly with temperature. Comparing Fig. 1(a), (b) and (c), the oxidation mass loss of TZM alloy plates is always higher than of the La-TZM alloy plates. This indicates that regardless of the high temperature exposure time, the oxidation mass loss of traditional TZM alloy is always higher than that of the La-TZM alloy, i.e. doping with La can considerably suppresses TZM alloys oxidation.

Tables 2 and 3 show the oxidation mass loss of La-TZM and TZM plates kept at 800 °C and 1000 °C for different time. The oxidation mass loss of the two kinds of samples is increasing with the

heating time. However, the mass loss of the La-TZM plates is less than the TZM alloy plates. For example, at 1000 °C the mass loss of La-TZM plates is 66.8%, 80.7% and 93.8% when heated for 10, 15 and 30 min, respectively. La doping can hinder the matrix erosion by oxygen during the high-temperature oxidation process, enhancing the oxidation resistance of TZM alloys.

3.2. Oxidation surface characterization of TZM alloy plates

3.2.1. Surface oxidation layer EDS analysis

Fig. 2 shows the EDS spectra of La-TZM and TZM alloy plates heated at 800 °C and 1000 °C. The existence of molybdenum oxide can be detected by calculating the content ratio of O and Mo atoms. In Fig. 2, the percentage ratios of O and Mo atoms on the surface of La-TZM and TZM alloy plates are 2.51 and 2.65 after 10 min oxidation at 800 °C, respectively. After 30 min at 800 °C, the ratios are 2.67 and 2.75, and then after 10 min oxidation at 1000 °C the ratios are 2.49 and 2.77. After oxidation the content ratios of O and Mo atoms in the surface layers of the La-TZM alloy plates are lower than the traditional TZM alloy plates, thus there is less MoO₃ due to lower oxygen uptake in the La-TZM alloy. This shows that La doping improves TZM alloy oxidation resistance.

3.2.2. Surface morphology

Fig. 3 shows SEM images of La-TZM and traditional TZM alloy plates heated at 800 °C and 1000 °C. Some bright spots are seen in all images of Fig. 3. Combined with the EDS analysis, it is clear that molybdenum oxides were generated, causing surface electrical conductivity reduction. Fig. 3(b) and (d) shows surface corrosion during the oxidation process in the form of lamellar slices, which obviously expand and fracture. In addition, the defect areas were oxidized more severely, and after 30 min of oxidation the lamellar molybdenum oxides were broken, causing the matrix to

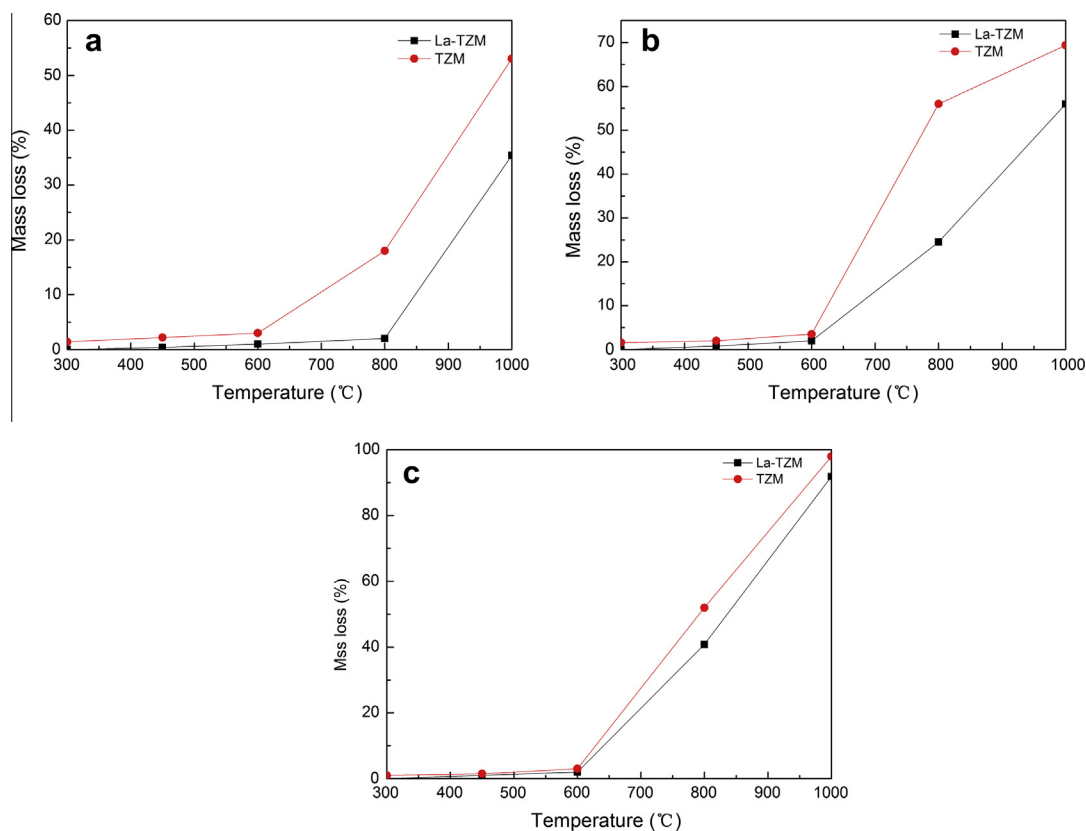


Fig. 1. Oxidation mass loss of the samples heated for: (a) 10 min, (b) 15 min and (c) 30 min.

Table 2

The mass loss of TZM alloy plates at 800 °C.

Heating temperature (°C)	Holding time (min)	Mass loss (%)	
		La-TZM #1-1	TZM #2-1
800	10	2	18
800	15	24.49	56
800	30	40.81	52

Table 3

The mass loss of TZM alloy plates at 1000 °C.

Heating temperature (°C)	Holding time (min)	Mass loss (%)	
		La-TZM #1-1	TZM #2-1
1000	10	35.42	53.06
1000	15	56	69.39
1000	30	91.83	97.95

be corroded even more (Fig. 3(f)). The surface of La-TZM alloy plates gradually corroded at different oxidation time in the form of lamellae. Compared with the traditional TZM alloy, La-TZM slices had less cavity defects in Fig. 3(a), (c) and (e), with only a few expanded slices after 15 min of oxidation at 1000 °C, seen in Fig. 3(i).

After 10 min of oxidation at 1000 °C, some flocculent oxides of molybdenum appeared on the samples surface in Fig. 3(g) and (h), and then disappeared after 15 min of oxidation, leaving the lamellar oxide layer in Fig. 3(i) and (j). However, for the traditional TZM alloy,

the flocculent oxides of molybdenum appeared on the samples surface after 15 min of oxidation at 800 °C in Fig. 3(d), and then disappeared, while the oxide layer fractured after 30 min of oxidation. Flocculent oxides of molybdenum appear on the surface of TZM alloy plates after 10 min of oxidation at 1000 °C, indicating that traditional TZM alloys are more easily oxidized.

3.2.3. Cross-sectional morphology

Fig. 4 shows cross-sectional SEM images of La-TZM and traditional TZM alloy plates heated at 800 °C and 1000 °C after 10 min. As seen in Fig. 4(b) and (d), after 10 min heating at 800 °C, the two kinds of alloy plates have thick oxide layer, thus the loose and lamellar morphology of molybdenum oxides is consistent with the surface images in Fig. 3. From these images once can see a compact oxide layer between the loose layer and the alloy matrix. After 10 min oxidation at 1000 °C, the loose and lamellar layer disappeared, leaving only the denser previously cracked oxide layer (Fig. 4(e) and (f)).

As seen in Fig. 4(a) and (c), the average thickness of loose oxide layer of La-TZM and traditional TZM alloy plates is 92 μm and 221 μm, respectively. The lamellar oxide layer of the TZM alloy plates is 2–3 times thicker than of the La-TZM alloy plates. From Fig. 4(e) and (f), the compact oxide layer of the La-TZM alloy plates is thicker than of the TZM alloy plates, which also indicates that the traditional TZM alloys are more easily oxidized.

3.3. Oxidation process analysis

Fig. 5 shows the TG–DTA curves of the La-TZM and the TZM alloy plates (samples #1-2 and #2-2) after comprehensive thermal

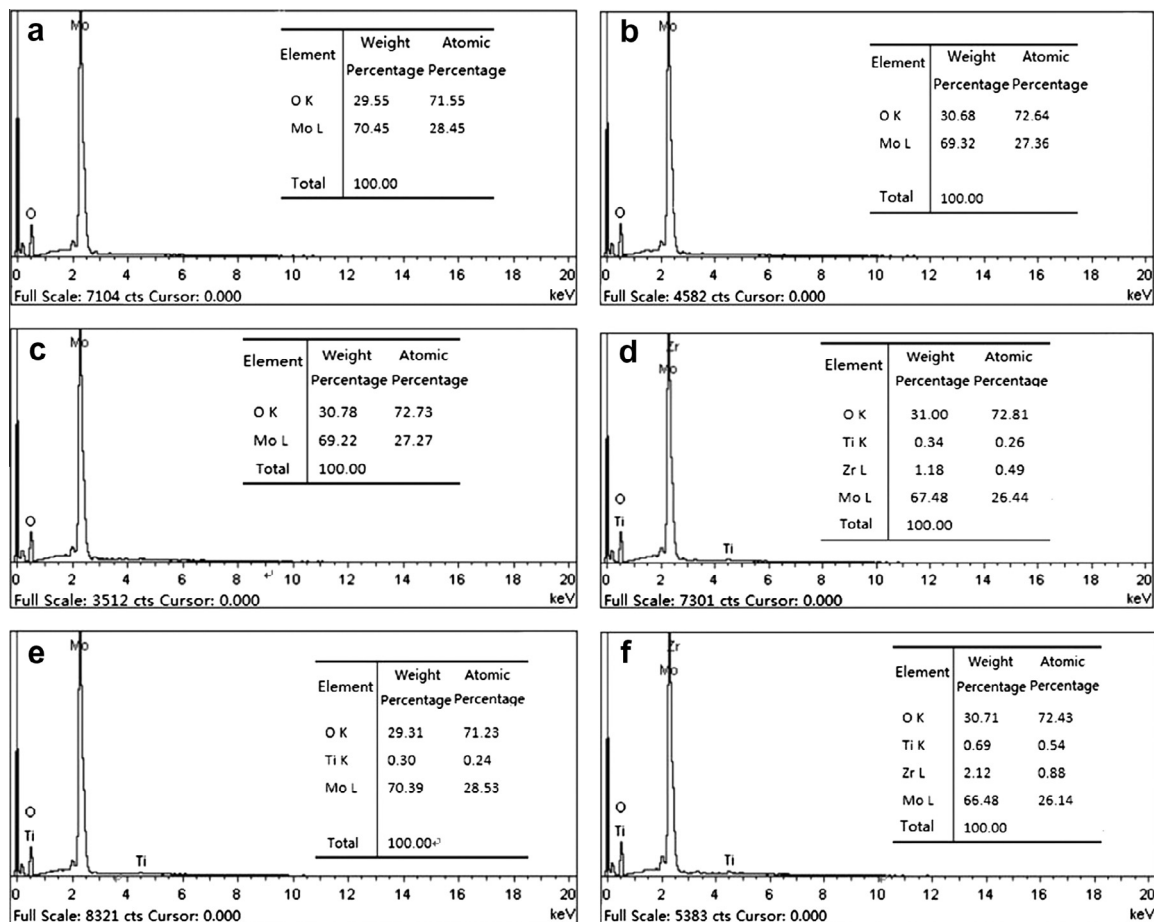


Fig. 2. EDS spectra of the samples oxidized at different temperature and time: (a) La-TZM, 800 °C, 10 min; (b) TZM, 800 °C, 10 min; (c) La-TZM, 800 °C, 30 min; (d) TZM, 800 °C, 30 min; (e) La-TZM, 1000 °C, 10 min; (f) TZM, 1000 °C, 10 min.

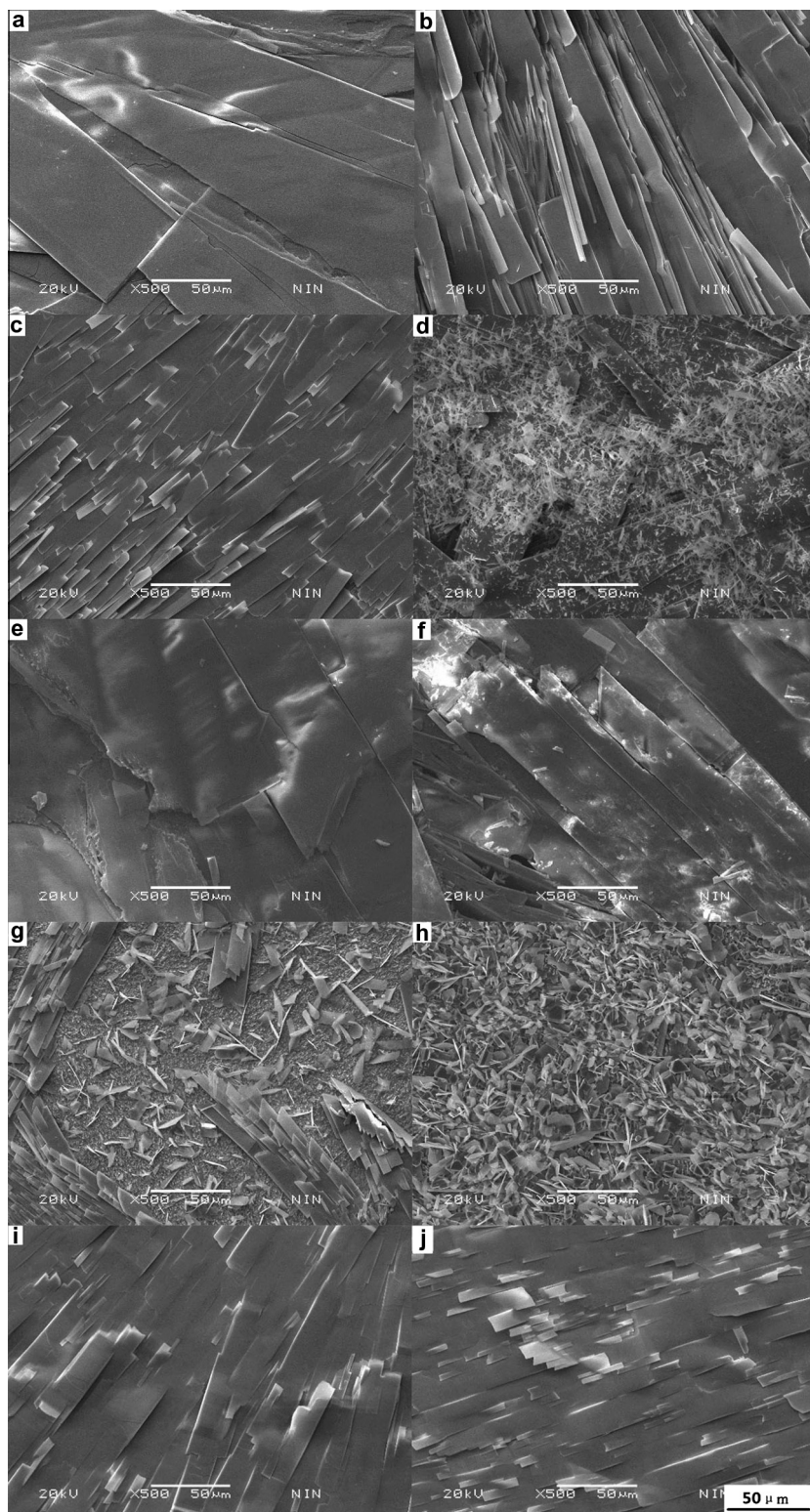


Fig. 3. SEM images of samples oxidized at different temperature and time: (a) La-TZM, 800 °C, 10 min; (b) TZM, 800 °C, 10 min; (c) La-TZM, 800 °C, 15 min; (d) TZM, 800 °C, 15 min; (e) La-TZM, 800 °C, 30 min; (f) TZM, 800 °C, 30 min; (g) La-TZM, 1000 °C, 10 min; (h) TZM, 1000 °C, 10 min; (i) La-TZM, 1000 °C, 15 min; (j) TZM, 1000 °C, 15 min.

analysis experiment. Based on the two TG curves, both samples have some gain of mass when heated at low temperatures. When heated to 850 °C, an exothermic peak appeared in the corresponding DTA curves with the sudden mass loss. Combined with the EDS analysis, the resultant MoO_3 is obviously volatile at this temperature. Comparing Fig. 5(a) and (b), there is a small exothermic peak

at 510 °C, and an obvious step rise in the TG curve. Based on the known TZM alloys oxidation kinetics, the oxidation reaction accelerated at this temperature with MoO_3 formation. However, a small exothermic peak at 460 °C in Fig. 5(b) manifests oxidation reaction aggravation at 460 °C. Comparing the two TG curves, the mass loss is 8.08% when heated at 1100 °C in Fig. 5(a), and 10.58% in Fig. 5(b),

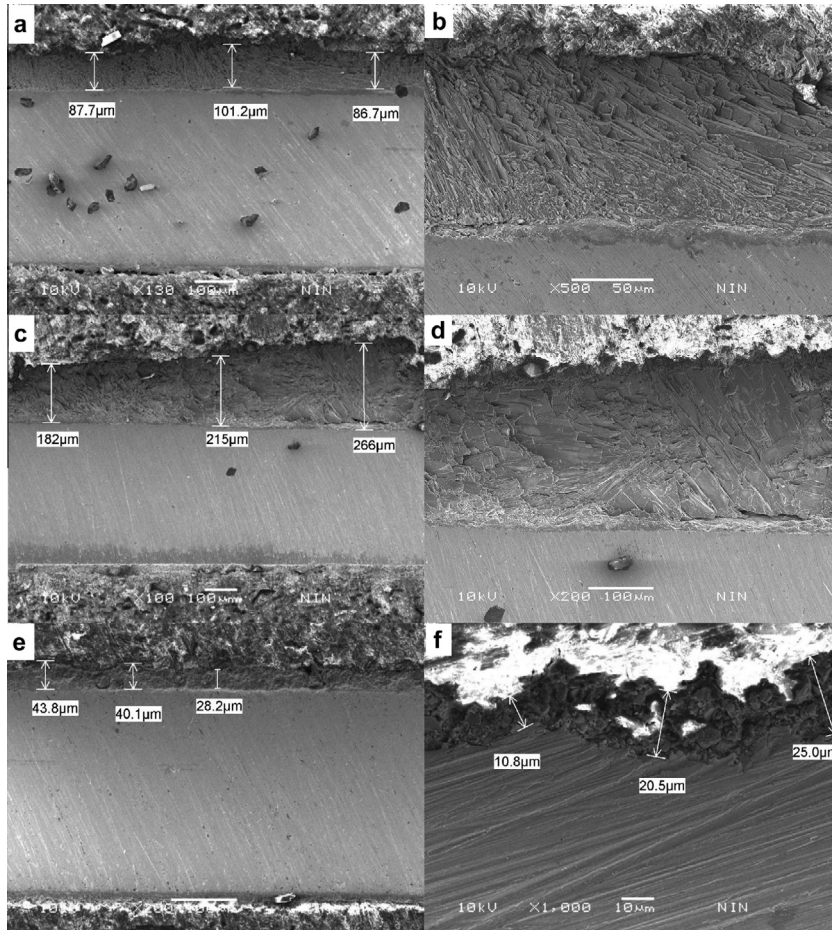


Fig. 4. Cross-sectional SEM images of samples oxidized at 800 °C and 1000 °C after 10 min: (a) (b) La-TZM, 800 °C, 10 min; (c) (d) TZM, 800 °C, 10 min; (e) La-TZM, 1000 °C, 10 min; (f) TZM, 1000 °C, 10 min.

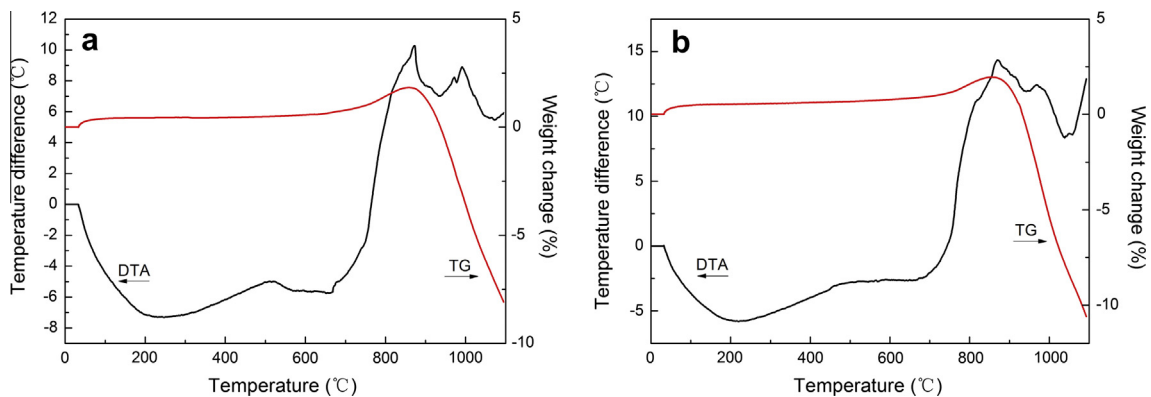


Fig. 5. TG-DTA curves of (a) La-TZM alloy and (b) TZM alloy.

indicating that sample #2-2 experienced a more serious volatilization. Compared with the traditional TZM alloys, La-TZM alloys have better oxidation resistance.

3.4. Oxidation mechanism

A protective layer can be formed on the TZM alloy plate surface by the 400–800 °C high-temperature oxidation. The protective layer is composed of MoO_3 , MoO_2 , other alloy oxide elements and a light-weight reinforced phase. However, increased oxidation time or temperature cause this layer to expand, fracture and

gradually get volatilized, allowing oxygen to corrode the matrix. La-doped TZM alloy microstructure schematic is shown in Fig. 6 [1], where due to a mix of the TZM alloy with the lanthanum nitrate solution, La exists in the form of La_2O_3 in the alloy. Since the La_2O_3 particles are smaller than the TZM alloy matrix grains, they fill up the spaces along the grain boundaries and pin in the voids of matrix, allowing for a denser microstructure organization. La element exists in the alloy, forming the second phase that has a dispersion strengthening effect, which improves the alloy durability. There exist lesser voids at surface and grain boundary, so that oxygen is hard to enter and corrode the matrix. On the other hand,

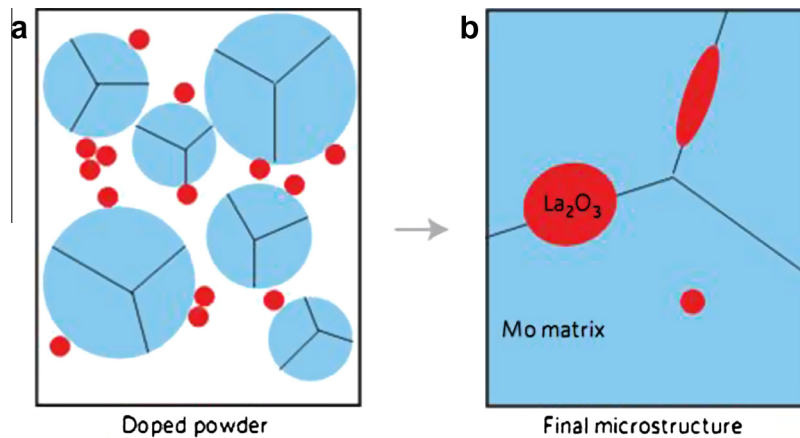


Fig. 6. Schematic of lanthanum element location in the La-TZM alloy: (a) initial microstructure; (b) final microstructure.

the laminated oxide layer covers the matrix surface, preventing further matrix oxidation. These can enhance the high-temperature oxidation resistance of the La-TZM alloy, so its oxidation mass loss is lower than the traditional TZM alloy.

4. Conclusions

- (1) After heating for a certain time, the traditional TZM alloy plates get oxidized in the flawed areas, such as grain boundaries and interfaces. Oxygen corrodes the matrix and the surround surface, generating an oxide layer. This layer is unstable, expands and fractures, causing further matrix oxidation and the obvious mass loss.
- (2) The rare earth element lanthanum doped TZM alloy has more compact organization due to the effects of tiny lanthanum oxide particles. Alloy oxide generated will be formed in the dense oxide layer on the substrate surface, which can effectively block the invasion of oxygen to the matrix, causing the improvement of the La-TZM alloy's oxidation resistance. Compared with the traditional TZM alloy, TZM alloy doped with La can rise the starting temperature of severe oxidation reaction by more than 50 °C and can effectively slow down the oxidation rate.
- (3) From the experiment, the lanthanum-doped TZM alloy has better durability and corrosion resistance, which can expand the application range of TZM alloys. This study of high-temperature oxidation resistance can provide guidance for

the follow-up experiments of improving the high-temperature oxidation resistance and anti-oxidation coating of TZM alloy.

Acknowledgments

This work was supported by the Major scientific and technological innovation project of Shaanxi province of China (S2011ZK1087), supported by Educational Commission of Shaanxi Province of China (12JK0431) and the Science and Technology Innovation Fund Project of the Western Metal Materials Co., Ltd (XBCL-1-06).

References

- [1] G. Liu, G.J. Zhang, F. Jiang, X.D. Ding, Y.J. Sun, J. Sun, E. Ma, *Nat. Mater.* 3544 (2013) 344–350.
- [2] S. Majumdar, I.G. Sharma, *Intermetallics* 19 (2011) 541–545.
- [3] S.P. Chakraborty, S. Banerjee, I.G. Sharma, A.K. Suri, *J. Nucl. Mater.* 403 (2010) 152–159.
- [4] S.P. Chakraborty, S. Banerjee, K. Singh, I.G. Sharma, A.K. Grover, A.K. Suri, *J. Mater. Proc. Technol.* 207 (2008) 240–247.
- [5] S. Majumdar, *Surf. Coat. Technol.* 206 (2012) 3393–3398.
- [6] J.R. DiStefano, B.A. Pint, J.H. DeVu, *Int. J. Refract. Metals Hard Mater.* 18 (2000) 237–243.
- [7] S. Majumdar, R. Kapoor, S. Raveendra, H. Sinha, I. Samajdar, P. Bhargav, J.K. Chakravartty, I.G. Sharma, A.K. Suri, *J. Nucl. Mater.* 385 (2009) 545–551.
- [8] G.R. Smolik, D.A. Petti, S.T. Schuetz, *J. Nucl. Mater.* 283–287 (2000) 1458–1462.
- [9] P. Hu, K.S. Wang, H.C. He, X.Q. Kang, H. Wang, P.Z. Wang, *Appl. Mech. Mater.* 320 (2013) 350–353.